Phenomenological study of two-meson couplings of Θ^+

Tetsuo Hyodo* and Atsushi Hosaka

Research Center for Nuclear Physics (RCNP), Ibaraki, Osaka 567-0047, Japan
(Dated: December 6, 2018)

We evaluate two-meson couplings of Θ^+, using experimental information of nucleon resonances decaying into $\pi\pi N$ channels, in which the two pions are in scalar- and vector-type correlations. We examine two assignments of spin and parity of $J^P = 1/2^+$ and $3/2^-$, for which the experimental spectra of known resonances with exotic baryons are properly reproduced by an octet-antidecuplet representation mixing scheme. With the obtained coupling constants, total cross sections of the reactions $\pi^- p \to K^- \Theta^+$ and $K^+ p \to \pi^+ \Theta^+$ are calculated. Substantial interference of two terms may occur in the reaction processes for the $J^P = 1/2^+$ case, whereas the interference effect is rather small for the $3/2^-$ case.

I. INTRODUCTION

Evidence for the existence of the exotic baryon Θ^+ [1] has been stimulating theoretical and experimental studies in hadron spectroscopy. The study of multiquark states in QCD will eventually lead to the understanding of the rich structure of hadronic matter. Recently, however, the existence of the Θ^+ has become controversial [2]. There are more than 10 experiments that indicate evidence of the Θ^+, whereas a similar number of experiments claim null results. In such a situation, confirmation of existence (or nonexistence) of the Θ^+ is urgent and crucially important. For this, it is strongly desired to clarify the reaction mechanism for the production of Θ^+. Among various possibilities, a particularly interesting property that is expected to be characteristic to exotic baryons is their strong coupling to two-meson states in transitions to an ordinary baryon. This is the subject we study in the present paper.

Studying two-meson coupling is important for several reasons. First, a heptaquark model has been proposed in the early stage of development to explain a light mass and a narrow decay width [3–7]. Although a quantitative study—in particular with a model of hadrons where Θ^+ is regarded as a bound state of $\pi K N$ system—does not work with the present knowledge of hadron interactions, a two-meson contribution to the self-energy of Θ^+ has been shown to be consistent with the expected pattern of the masses of the antidecuplet members [8].

Second, the importance of two-meson coupling has been implied from an empirical observation of the extended OZI rule [9]. The dominance of connected quark lines favors creation of a $q\bar{q}$ pair in the transition of $\Theta^+(qqqq\bar{q}) \to N(qqq)$, which is naturally associated with the coupling to two mesons, whereas a coupling to a single meson is suppressed.

Finally, two-meson coupling plays an important role in reaction studies. Without two-meson coupling, all the

amplitudes for Θ^+ production are proportional to the $\Theta^+ K N$ coupling, which is fixed by the very small decay width of the Θ^+. However, two-meson coupling is determined from other source as we will see in the following, independently of the $\Theta^+ K N$ coupling. Therefore, even with the extremely narrow width of Θ^+, a sizable cross section can be obtained with two-meson coupling.

In Ref. [8], an analysis of the two-meson coupling is performed in the study of the self-energy of the Θ^+, assuming that $J^P = 1/2^+$ with $N(1710)$ in the same antidecuplet ($\overline{\mathbf{10}}$). Since the Θ^+ cannot decay into $K\pi N$ channel, the coupling constants are determined from the N^* decay into the $\pi\pi N$ channel and flavor SU(3) symmetry. Two types of Lagrangians are found to be important for the self-energy of the baryon antidecuplet. It is also shown that the two-meson contribution is indeed dominant over a single-meson contribution. However, the assumption of pure $\overline{\mathbf{10}}$ may not be the case in reality.

This point is clarified in Ref. [10], where we study the phenomenology of flavor partners for the Θ^+. We assign the masses of experimentally known particles in an octet-antidecuplet mixing scheme, finding good fits for $J^P = 1/2^+$ and $3/2^-$. The decay width of the Θ^+ is also evaluated in the same scheme, and the $J^P = 3/2^-$ case naturally explains the narrow width, in accordance with the quark model estimation [11]. In both J^P cases, we obtain relatively large mixing angles, which implies the importance of the representation mixing.

Hence, combining these two findings, we calculate the two-meson couplings including the representation mixing. First we determine the coupling constants of $N^* \to \pi\pi N$ from the experimental widths and separate the $\overline{\mathbf{10}}$ component from the $\mathbf{8}$ component. Then, by using SU(3) symmetry, the coupling constants of $\Theta K\pi N$ can be determined for $J^P = 1/2^+$ and $3/2^-$, including representation mixing of $\mathbf{8}$ and $\overline{\mathbf{10}}$. We focus on the decay channels in which the two pions are correlated in scalar-isoscalar and vector-isovector channels, which are the main decay modes of the resonances and play a dominant role in the Θ^+ self-energy [8].

As an application of the effective Lagrangians, we perform the analysis of the $\pi^- p \to K^- \Theta^+$ and $K^+ p \to$

*Electronic address: hyodo@rcnp.osaka-u.ac.jp

$\pi^+\Theta^+$ reactions. These reactions were studied using effective Lagrangian approaches [12–15]. Experiments for $\pi^- p \to K^- \Theta^+$ have been performed at KEK [16], and a high-resolution experiment for the $K^+ p \to \pi^+ \Theta^+$ reaction is ongoing. We can compare the results with these experiments.

This paper is organized as follows. In the next section, we show the framework of representation mixing and relevant experimental information of nucleon decay. In Sec. III, the effective interaction Lagrangians for nucleons and for the antidecuplet are introduced for both $J^P = 1/2^+$ and $3/2^-$ cases. The coupling constants are determined in Sec. IV by considering the decay widths of N^* resonances and the self-energy of the Θ^+. With the effective Lagrangians, the reaction processes $\pi^- p \to K^- \Theta^+$ and $K^+ p \to \pi^+ \Theta^+$ are analyzed in Sec. V. The final section is devoted to a summary.

II. REPRESENTATION MIXING SCHEME AND EXPERIMENTAL INFORMATION

Let us briefly review the previous study of representation mixing [10] and summarize the experimental decays of nucleon resonances. We have performed a phenomenological analysis on the exotic particles using flavor SU(3) symmetry. It is found that the masses of $\Theta(1540)$ and $\Xi_{3/2}(1860)$ are well fitted in an antidecuplet ($\overline{\mathbf{10}}$) representation which mixes with an octet ($\mathbf{8}$), with known baryon resonances of $J^P = 1/2^+$ or $3/2^-$. The $1/2^-$ case gives too large a decay width for the Θ^+, and not enough resonances are well established for $3/2^+$ to complete the analysis. Under the representation mixing, the physical nucleon states are defined as

$$\begin{aligned}
| N_1 \rangle &= | \mathbf{8}, N \rangle \cos\theta_N - | \overline{\mathbf{10}}, N \rangle \sin\theta_N, \\
| N_2 \rangle &= | \overline{\mathbf{10}}, N \rangle \cos\theta_N + | \mathbf{8}, N \rangle \sin\theta_N.
\end{aligned} \tag{1}$$

Two states N_1 and N_2 represents $N(1440)$ and $N(1710)$ for the $1/2^+$ case and $N(1520)$ and $N(1700)$ for the $3/2^-$ case. The mixing angles θ_N can be determined by experimental spectra of known resonances as

$$\theta_N = 29° \quad \text{for } J^P = 1/2^+ , \tag{2}$$

$$\theta_N = 33° \quad \text{for } J^P = 3/2^- . \tag{3}$$

Both angles are close to the ideal mixing $\theta_N \sim 35.2°$, in which the nucleon states are classified by the number of strange quarks (antiquarks). In other words, states are well mixed and the effect of mixing of states is important.

Using these mixing angles and decay widths of nucleon resonances ($\Gamma_{N^* \to \pi N}$), we can calculate the decay width of Θ ($\Gamma_{\Theta \to KN}$) through the SU(3) relation between the coupling constants

$$g_\Theta = \sqrt{6}(g_{N_2} \cos\theta_N - g_{N_1} \sin\theta_N),$$

where g_Θ, g_{N_1}, and g_{N_2} are the coupling constants of Θ and nucleon resonances. With the known coupling
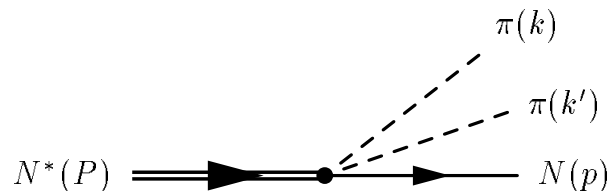

FIG. 1: Feynman diagram for the three-body decay of the N^* resonance.

TABLE I: Experimental information of two-pion decay of nucleon resonances. "Scalar" represents the mode $\pi\pi(I = 0, s$ wave$)N$ and "Vector" means $\pi\pi(I = 1, p$ wave$)N$ mode. Values in parenthesis are averaged over the interval quoted in PDG [17].

J^P	State	Γ_{tot} [MeV]	Scalar [%]	Vector [%]
$1/2^+$	N(1440)	350	5-10(7.5)	<8
	N(1710)	100	10-40(25)	5-25(15)
$3/2^-$	N(1520)	120	10-40(25)	15-25(20)
	N(1700)	100	< 85-95^a	<35

^{a}The scalar decay of $N(1700)$ is taken from the total branching ratio to the $\pi\pi N$ channel.

constants g_{N_1} and g_{N_2}, we obtained $\Gamma_\Theta \sim 30$ MeV for $J^P = 1/2^+$ and $\Gamma_\Theta \sim 3$ MeV for $J^P = 3/2^-$. Here we extend this approach to the three-body decay, as shown in Fig. 1.

In Table I, we show the experimental information of the decay pattern of the nucleon resonances $N^* \to \pi\pi N$ taken from the Particle Data Group (PDG) [17]. For convenience, we refer to $\pi\pi(I = 0, s$ wave$)N$ and $\pi\pi(I = 1, p$ wave$)N$ modes as "scalar" (s) and "vector" (v), respectively. There is no information for the scalar decay of $N(1700)$. PDG only shows the fraction decaying via the $\pi\pi N$ mode (85-95%) and an upper bound for ρN mode ($<35\%$), although several intermediate states including $\pi\pi(I = 0, s$ wave$)N$ are shown in the table. For the estimation of the coupling constants, we adopt the total branching ratio to $\pi\pi N$ channel as the upper limit of the branch for $\pi\pi(I = 0)N$ state, $BR_{N(1700) \to \pi\pi(I=0)N} < 85$-95%.

III. EFFECTIVE INTERACTION LAGRANGIANS

Here we write down the effective Lagrangians that account for the interactions in the present analysis. We need two steps, namely, the extraction of the $\overline{\mathbf{10}}$ component from the $N^* \to \pi\pi N$ decay and the extrapolation to the $\Theta \pi K N$ channel. Lagrangians for nucleons will be used for the former purpose; the Lagrangians for the antidecuplet will tell us the SU(3) relation between channels

in the multiplet.

In general, for an $N^* \to \pi\pi N$ vertex with an N^* in octet or antidecuplet representations, there are several structures of interaction Lagrangians that are SU(3) symmetric. However, for octet N^*, information of other channels are not relevant here, because we do not want to study other channels. Therefore, we write down only the $N^*\pi\pi N$ channels, instead of writing down all possible Lagrangians.

Using the partial decay widths of the two nucleon resonances $\Gamma_i^{s,v}$, we determine the absolute values of the coupling constants $|g_i^{s,v}|$, where superscripts s and v stand for the scalar- and vector-type correlations of two mesons. From them, we can obtain the antidecuplet and octet components of the coupling constants as

$$g^{s,v}(\overline{10}) = -|g_1^{s,v}|\sin\theta_N \pm |g_2^{s,v}|\cos\theta_N,$$
$$g^{s,v}(8) = |g_1^{s,v}|\cos\theta_N \pm |g_2^{s,v}|\sin\theta_N, \qquad (4)$$

based on Eq. (1). Since the relative phase of the two coupling constants cannot be determined, the $\pm$ sign appears. Here we use θ_N obtained from the mass spectra as shown in Eqs. (2) and (3). When the coupling constants have experimental uncertainties, we vary them within the region and check the minimum and maximum of corresponding values of $g^{s,v}(\overline{10})$.

A. Lagrangians for nucleons with $J^P = 1/2^+$

Let us consider the $J^P = 1/2^+$ case. The interaction Lagrangians for nucleons can be written as

$$\mathcal{L}_i^s = \frac{g_i^s}{2\sqrt{2}f}\overline{N}_i^*\boldsymbol{\pi}\cdot\boldsymbol{\pi}N + \text{h.c.} \qquad (5)$$

and

$$\mathcal{L}_i^v = i\frac{g_i^v}{4\sqrt{2}f^2}\overline{N}_i^*(\boldsymbol{\pi}\cdot\overleftrightarrow{\partial\!\!\!/}\boldsymbol{\pi})N + \text{h.c.}$$
$$= i\frac{g_i^v}{4\sqrt{2}f^2}\overline{N}_i^*(\boldsymbol{\pi}\cdot\partial\!\!\!/\boldsymbol{\pi} - \partial\!\!\!/\boldsymbol{\pi}\cdot\boldsymbol{\pi})N + \text{h.c.}, \qquad (6)$$

where $f = 93$ MeV is the pion decay constant, $g_i^{s,v}$ are dimensionless coupling constants, and h.c. stands for the hermitian conjugate. Subscript $i = 1, 2$ denotes the two nucleons $N(1440)$ and $N(1710)$, respectively. The numerical factors are chosen such that the coupling constants $g_i^{s,v}$ should be consistent with the Lagrangians for the antidecuplet, which will be given later. For nucleon, N^*, and pion fields, we adopt the convention

$$N = \begin{pmatrix} p \\ n \end{pmatrix}, \quad N_i^* = \begin{pmatrix} p_i^* \\ n_i^* \end{pmatrix}, \quad \boldsymbol{\pi} = \begin{pmatrix} \pi^0 & \sqrt{2}\pi^+ \\ \sqrt{2}\pi^- & -\pi^0 \end{pmatrix}. \qquad (7)$$

B. Lagrangians for the antidecuplet with $1/2^+$

To connect the coupling constant of the process $N^*\pi\pi N$ to that of $\Theta K\pi N$, we write down the interaction Lagrangian for the antidecuplet. Flavor SU(3) structure of these terms are studied in Ref. [8]. In the present case, for the scalar-type correlation, we have

$$\mathcal{L}_{1/2^+}^s = \frac{g_{1/2^+}^s}{2f}\overline{P}_{ijk}\epsilon^{lmk}\phi_l{}^a\phi_a{}^i B_m{}^j + \text{h.c.}, \qquad (8)$$

whereas for the vector-type correlation, we have

$$\mathcal{L}_{1/2^+}^v = i\frac{g_{1/2^+}^v}{4f^2}\overline{P}_{ijk}\epsilon^{lmk}\gamma^\mu(\partial_\mu\phi_l{}^a\phi_a{}^i - \phi_l{}^a\partial_\mu\phi_a{}^i)B_m{}^j + \text{h.c.} \qquad (9)$$

In Eqs. (8) and (9), the coupling constants are for the antidecuplet baryon, which corresponds to Eq. (4). These Lagrangians correspond to $\mathcal{L}^{8s}$ and $\mathcal{L}^{8a}$ in Ref. [8]. The octet meson (baryon) field ϕ (B) and the antidecuplet baryon field P are defined as

$$\phi = \begin{pmatrix} \frac{1}{\sqrt{2}}\pi^0 + \frac{1}{\sqrt{6}}\eta & \pi^+ & K^+ \\ \pi^- & -\frac{1}{\sqrt{2}}\pi^0 + \frac{1}{\sqrt{6}}\eta & K^0 \\ K^- & \overline{K}^0 & -\frac{2}{\sqrt{6}}\eta \end{pmatrix}, \qquad (10)$$

$$B = \begin{pmatrix} \frac{1}{\sqrt{2}}\Sigma^0 + \frac{1}{\sqrt{6}}\Lambda & \Sigma^+ & p \\ \Sigma^- & -\frac{1}{\sqrt{2}}\Sigma^0 + \frac{1}{\sqrt{6}}\Lambda & n \\ \Xi^- & \Xi^0 & -\frac{2}{\sqrt{6}}\Lambda \end{pmatrix}, \qquad (11)$$

$$P^{333} = \sqrt{6}\,\Theta_{10}^+, \quad P^{133} = \sqrt{2}\,N_{10}^0,$$
$$P^{233} = -\sqrt{2}\,N_{10}^+, \quad P^{113} = \sqrt{2}\,\Sigma_{10}^-,$$
$$P^{123} = -\Sigma_{10}^0, \quad P^{223} = -\sqrt{2}\,\Sigma_{10}^+,$$
$$P^{111} = \sqrt{6}\,\Xi_{10}^{--}, \quad P^{112} = -\sqrt{2}\,\Xi_{10}^-,$$
$$P^{122} = \sqrt{2}\,\Xi_{10}^0, \quad P^{222} = -\sqrt{6}\,\Xi_{10}^+. \qquad (12)$$

Note that the coefficients for $N^*\pi\pi N$ in the expansion of the Lagrangians are the same as Eqs. (5) and (6), respectively. This means that the normalization of the coupling constants in both Lagrangians are the same.

There is another Lagrangian for the scalar-type correlation $\mathcal{L}^{27}$ [8]. However, the contribution of this term can be expressed by the following parametrization:

$$a\mathcal{L}^{8s} + b\mathcal{L}^{27}, \quad b = -\tfrac{5}{4}(1-a), \qquad (13)$$

with $g^{8s} = g^{27}$. The ratio of $\mathcal{L}^{8s}$ and $\mathcal{L}^{27}$ is controlled by the parameter a, without changing the total coupling constant of $N^*\pi\pi N$. The important point is that this combination of the two Lagrangians also does not change the $\Theta K\pi N$ channel, as we can see in the table in Ref. [8]. Therefore, in the present purpose, it is sufficient to consider the Lagrangians (8) and (9).

C. Lagrangians for nucleons with $J^P = 3/2^-$

We express the spin $3/2$ baryons as Rarita-Schwinger fields B^μ [18]. The effective Lagrangians can be written

as

$$\mathcal{L}_i^s = i\frac{g_i^s}{4\sqrt{2}f^2}\overline{N}_i^{*\mu}\partial_\mu(\boldsymbol{\pi}\cdot\boldsymbol{\pi})N + \text{h.c.}$$

$$= i\frac{g_i^s}{4\sqrt{2}f^2}\overline{N}_i^{*\mu}(\partial_\mu\boldsymbol{\pi}\cdot\boldsymbol{\pi} + \boldsymbol{\pi}\cdot\partial_\mu\boldsymbol{\pi})N + \text{h.c.} \quad (14)$$

and

$$\mathcal{L}_i^v = i\frac{g_i^v}{4\sqrt{2}f^2}\overline{N}_i^{*\mu}(\boldsymbol{\pi}\cdot\overleftrightarrow{\partial}_\mu\boldsymbol{\pi})N + \text{h.c.} \quad (15)$$

Here $i = 1, 2$ denotes the two nucleons $N(1520)$ and $N(1700)$, respectively. Notice that a derivative of meson field is needed for the scalar Lagrangian whose Dirac index is to be contracted with that of Rarita-Schwinger field. Since the flavor structure of these Lagrangians is the same as in Eqs. (5) and (6), we will have the same coefficients up to the coupling factors. The antidecuplet component of the coupling constants can be determined as in Eq. (4).

D. Lagrangians for the antidecuplet with $3/2^-$

We write the Lagrangians for the antidecuplet as a straightforward extension of those in $1/2^+$ case:

$$\mathcal{L}_{3/2^-}^s = i\frac{g_{3/2^-}^s}{4f^2}\overline{P}_{ijk}^\mu \epsilon^{lmk}\partial_\mu(\phi_l{}^a\phi_a{}^i)B_m{}^j + \text{h.c.} \quad (16)$$

while for the vector type correlation we have

$$\mathcal{L}_{3/2^-}^v = i\frac{g_{3/2^-}^v}{4f^2}\overline{P}_{ijk}^\mu \epsilon^{lmk}(\partial_\mu\phi_l{}^a\phi_a{}^i - \phi_l{}^a\partial_\mu\phi_a{}^i)B_m{}^j + \text{h.c.} \quad (17)$$

Here the flavor structure is the same as in Eq. (9).

IV. NUMERICAL RESULTS FOR THE COUPLING CONSTANTS

To study the coupling constants, let us start with the decay width of a resonance into two mesons and one baryon, which is given by

$$\Gamma_{\text{BMM}} = \int \frac{d^3p}{(2\pi)^3}\frac{M}{E(p)}\int\frac{d^3k}{(2\pi)^3}\frac{1}{2\omega(k)}\int\frac{d^3k'}{(2\pi)^3}\frac{1}{2\omega'(k')}$$
$$\times \overline{\Sigma}\Sigma|t(\omega,\omega',\cos\theta)|^2(2\pi)^4\delta^{(4)}(P-p-k-k')$$
$$= \frac{M}{16\pi^3}\int_{\omega_{\text{min}}}^{\omega_{\text{max}}}d\omega\int_{\omega'_{\text{min}}}^{\omega'_{\text{max}}}d\omega'$$
$$\times \overline{\Sigma}\Sigma|t(\omega,\omega',a)|^2\Theta(1-a^2), \quad (18)$$

with

$$\omega_{\text{min}} = m,$$
$$\omega_{\text{max}} = \frac{M_R^2 - M^2 - 2Mm}{2M_R},$$
$$a = \frac{(M_R - \omega - \omega')^2 - M^2 - |\boldsymbol{k}|^2 - |\boldsymbol{k}'|^2}{2|\boldsymbol{k}||\boldsymbol{k}'|},$$

where we assign the momentum variables $P = (M_R, \mathbf{0})$, $k = (\omega, \boldsymbol{k})$, $k' = (\omega', \boldsymbol{k}')$, and $p = (E, \boldsymbol{p})$ as in Fig. 1; M_R, M, and m are the masses of the resonance, baryon, and mesons, respectively; and θ is the angle between the momenta $\boldsymbol{k}$ and $\boldsymbol{k}'$. The on-shell energies of particles are given by $\omega = \sqrt{m^2 + \boldsymbol{k}^2}$, $\omega' = \sqrt{m^2 + (\boldsymbol{k}')^2}$, and $E = \sqrt{M^2 + \boldsymbol{p}^2}$; Θ denotes the step function; and $\overline{\Sigma}\Sigma$ stands for the spin sum of the fermion states.

In the following, we evaluate the squared amplitude $\overline{\Sigma}\Sigma|t(\omega, \omega', \cos\theta)|^2$ for the $N^* \to \pi\pi N$ decay in the nonrelativistic approximation. For the $1/2^+$ case, from Eq. (5), the scalar Lagrangian gives the term

$$\overline{\Sigma}\Sigma|t_{1/2^+}^s|^2 = 3\left(\frac{g_{1/2^+}^s}{2f}\right)^2\frac{E+M}{2M}. \quad (19)$$

Note that we include the normalization factor $(E + M)/2M$ to be consistent with the other amplitude, although the effect of this factor is small (of the order of a few percent) in the results.

For the vector-type coupling, we insert the vector meson propagator to account for the ρ meson correlation [8], as shown in Fig. 2. Then the squared amplitude becomes

$$\overline{\Sigma}\Sigma|t_{1/2^+}^v|^2 = 6\left(\frac{g_{1/2^+}^v}{4f^2}\right)^2\frac{1}{2M}\Big\{(E+M)(\omega-\omega')^2$$
$$+ 2(|\boldsymbol{k}|^2 - |\boldsymbol{k}'|^2)(\omega - \omega')$$
$$+ (E-M)(\boldsymbol{k}-\boldsymbol{k}')^2\Big\}$$
$$\times \left|\frac{-m_\rho^2}{s'-m_\rho^2+im_\rho\Gamma(s')}\right|^2, \quad (20)$$

where m_ρ is the mass of ρ meson, $s' = (k+k')^2$, and $\Gamma(s')$ is the energy-dependent width given by

$$\Gamma(s') = \Gamma_\rho \times \left(\frac{p_{\text{cm}}(s')}{p_{\text{cm}}(m_\rho^2)}\right)^3,$$

with the three-momentum of the final particles in the ρ rest frame given by

$$p_{\text{cm}}(s') = \begin{cases} \frac{\lambda^{1/2}(s',m_\pi^2,m_\pi^2)}{2\sqrt{s'}} & \text{for } s' > 4m_\pi^2, \\ 0 & \text{for } s' \leqslant 4m_\pi^2, \end{cases}$$

and $\lambda(a, b, c)$ is the Källen function. Note that in Eq. (20) we take the terms up to next to leading order in the nonrelativistic expansion, since the leading order term $(\omega - \omega')$ appears as the difference of two energies, which can be zero.
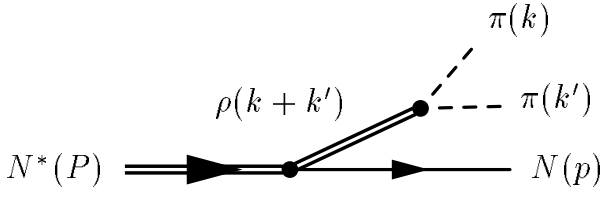
The squared amplitudes for $J^P = 3/2^-$ can be ob-

FIG. 2: Three-body decay of the N^* resonance with insertion of the vector meson propagator.

tained in a similar way:

$$\overline{\Sigma}\Sigma|t^s_{3/2^-}|^2 = \left(\frac{g^s_{3/2^-}}{4f^2}\right)^2 (\boldsymbol{k} + \boldsymbol{k}')^2 \frac{E+M}{2M}, \tag{21}$$

$$\overline{\Sigma}\Sigma|t^v_{3/2^-}|^2 = 2\left(\frac{g^v_{3/2^-}}{4f^2}\right)^2 (\boldsymbol{k} - \boldsymbol{k}')^2 \frac{E+M}{2M}$$
$$\times \left|\frac{-m^2_\rho}{s' - m^2_\rho + im_\rho\Gamma(s')}\right|^2. \tag{22}$$

A. Numerical result for the $J^P = 1/2^+$ case

Now we evaluate the coupling constants numerically. Using the averaged values in Table I, we obtain the coupling constants g^s_i and g^v_i for these channels:

$$|g^s_{N(1440)}| = 4.28, \qquad |g^v_{N(1440)}| < 3.68, \tag{23}$$
$$|g^s_{N(1710)}| = 1.84, \qquad |g^v_{N(1710)}| = 0.31. \tag{24}$$

By substituting them into Eq. (4) (but suppressing the label $\overline{\mathbf{10}}$ for simplicity), the antidecuplet components are extracted as

$$|g^s_{1/2^+}| = 0.47, \quad 3.68, \tag{25}$$

where two values correspond to the results with different relative phases between the two coupling constants. For $|g^v_{1/2^+}|$, only the upper bound is given for $N(1440)$; therefore we can not fix the central value.

When we take into account the experimental uncertainties in branching ratio, the antidecuplet components can vary within the following ranges:

$$0 < |g^s_{1/2^+}| < 1.37, \qquad 0 < |g^v_{1/2^+}| < 2.14,$$
$$2.72 < |g^s_{1/2^+}| < 4.42,$$

including both cases for the phase. These uncertainties are also shown by the vertical bar in Fig. 3, with the horizontal bars being the result with the averaged value in Eq. (25).

Now let us consider the phenomenological implication of this result. In the study of self-energy [8], the coupling
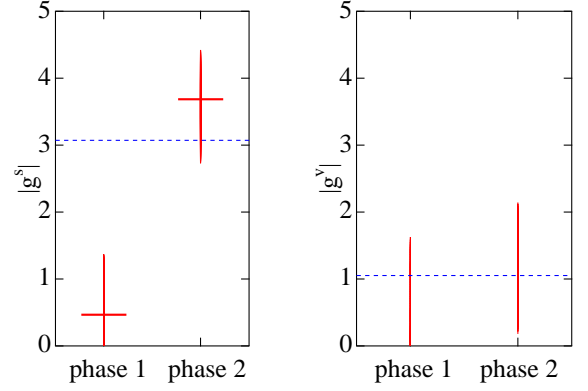

FIG. 3: (Color online) Numerical results for the coupling constants with $J^P = 1/2^+$. The two choices of the relative phase between coupling constants are marked as "phase 1" and "phase 2". Allowed regions of the coupling constants are shown by the vertical bar. Horizontal bars represent the results obtained with the averaged values, which are absent for the vector case. Horizontal dashed lines show the upper limits of the coupling constants derived from the self-energy $|\mathrm{Re}\Sigma| < 200$ MeV.

constants have been derived by assuming that the Θ^+ belongs to a pure antidecuplet together with $N(1710)$, where we have determined $|g^s_{1/2^+}| = 1.88$ and $|g^v_{1/2^+}| = 0.315$ [essentially the same as values in Eq. (24)]. In the calculation of the self-energy of Θ^+, the effect of the mixing only changes the coupling constants, by neglecting the small contribution from $\mathcal{L}^{27}$. In this case, the Θ^+ self-energy with the new coupling constants can be written as

$$\Sigma^s_{\Theta^+}(g^s_{1/2^+}) = \Sigma^s_{\Theta^+}(1.88) \times \frac{|g^s_{1/2^+}|^2}{1.88^2}, \tag{26}$$

$$\Sigma^v_{\Theta^+}(g^v_{1/2^+}) = \Sigma^v_{\Theta^+}(0.315) \times \frac{|g^v_{1/2^+}|^2}{0.315^2}. \tag{27}$$

The real parts of the self-energy depend on the initial energy and the cutoff value of the loop integral. We have estimated $\mathrm{Re}\Sigma^s_{\Theta^+}(g = 1.88) \sim -75$ MeV and $\mathrm{Re}\Sigma^v_{\Theta^+}(g = 0.315)) \sim -18$ MeV for an initial energy of 1540-1700 MeV and with a cutoff of 700-800 MeV. Using Eqs. (26) and (27) with the values of Eq. (25), we obtain

$$\Sigma^s_{\Theta^+} = -287, \quad -4.7 \text{ MeV}, \quad 0 > \Sigma^v_{\Theta^+} > -770 \text{ MeV}. \tag{28}$$

The sum of these values are the contribution to the self-energy of Θ^+ from the two-meson cloud. Naively, we expect that it should be of the order of 100 MeV, at most $\sim 20\%$ of the total energy [8, 19]. From this consideration, we adopt the condition that the magnitude of one of the contributions should not exceed 200 MeV: $|\mathrm{Re}\Sigma^v_{\Theta^+}| < 200$.

For the scalar coupling, this condition is satisfied when
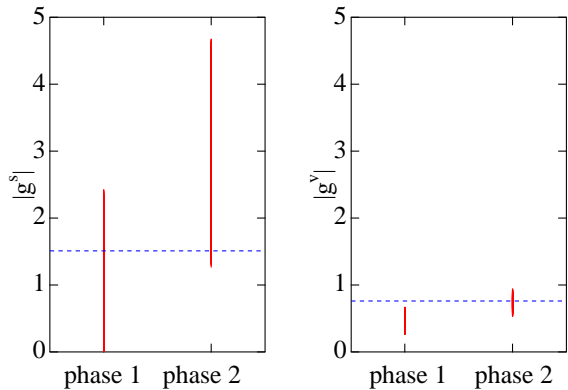
$$|g^s_{1/2^+}| < 3.07. \tag{29}$$

FIG. 4: (Color online) Numerical results for the coupling constants with $J^P = 3/2^-$. The two choices of the relative phase between coupling constants are marked as "phase 1" and "phase 2". Allowed regions of the coupling constants are shown by the vertical bar. Horizontal dashed lines show the upper limit of the coupling constants derived from the self-energy $|\mathrm{Re}\Sigma| < 200$ MeV.

Therefore, we can exclude the choice of "phase 2" in Fig. 3. In the same way, the upper limit of $|g^v_{1/2^+}|$ should be imposed as

$$|g^v_{1/2^+}| < 1.05 \tag{30}$$

to be consistent with the condition $|\mathrm{Re}\Sigma^v_{\Theta^+}| < 200$ MeV. This is compatible with Eq. (25), although Eq. (30) gives a more stringent constraint. These upper limits are also shown in Fig. 3 by the dashed lines.

B. Numerical result for the $J^P = 3/2^-$ case

Now we consider the $J^P = 3/2^-$ case. Using the central values in Table I, we obtain the coupling constants g^s_i and g^v_i for these channels:

$$|g^s_{N(1520)}| = 3.56, \qquad |g^v_{N(1520)}| = 1.11, \tag{31}$$
$$|g^s_{N(1700)}| < 2.66, \qquad |g^v_{N(1700)}| < 0.32. \tag{32}$$

In this case, with the same reason as in the vector coupling for the $1/2^+$ case, the central value cannot be determined. Experimental uncertainties allows the antidecuplet components to vary within the following ranges:

$$0 < |g^s_{3/2^-}| < 4.68, \qquad 0.25 < |g^v_{3/2^-}| < 0.94, \tag{33}$$

including both cases for the phase. The result are shown by the vertical bars in Fig. 4.

It is worth noting that the region of $|g^v_{3/2^-}|$ does not reach zero, even though the $|g^v_{N(1700)}|$ can be zero. The condition for $g^{s,v}(\overline{\mathbf{10}}) = 0$ leads to

$$\frac{|g^{s,v}_2|}{|g^{s,v}_1|} = \tan\theta_N \sim \begin{cases} 0.55 & \text{for } 1/2^+, \\ 0.65 & \text{for } 3/2^-. \end{cases} \tag{34}$$

This means that $g^{s,v}(\overline{\mathbf{10}})$ becomes zero only if the condition (34) is satisfied within the uncertainty of coupling constants.

We can also estimate the magnitude of the self-energy, by substituting the squared amplitudes for $3/2^-$ case in the formulas of the self-energy shown in Ref. [8]. For $|g^s_{3/2^-}| = 4.17$, we estimate the real part of the self-energy as -1518 MeV for an initial energy of 1540-1700 MeV and a cutoff of 700-800 MeV. This huge self-energy for $3/2^-$ case is due to the p-wave nature of the two-meson coupling, namely, the existence of a momentum variable in the loop integral. A similar large self-energy was observed when the self-energy is calculated with the chiral Lagrangian in Ref. [8]. Thus, to have some reasonable values for the self-energy $|\mathrm{Re}\Sigma^s_{\Theta^+}| < 200$ MeV,

$$|g^s_{3/2^-}| < 1.51. \tag{35}$$

In the same way, for the vector term with $|g^v_{3/2^-}| = 0.61$, we estimate the real part of the self-energy as -130 MeV. In this case, the self-energy is suppressed by the vector meson propagator. The use of small number 0.61 for the coupling constant also accounts for the small value of the self-energy. The condition of the self-energy $|\mathrm{Re}\Sigma^v_{\Theta^+}| < 200$ MeV gives the constraints

$$|g^v_{3/2^-}| < 0.76. \tag{36}$$

Both upper limits (35) and (36) are indicated by horizontal dashed lines in Fig. 4.

V. ANALYSIS OF THE MESON-INDUCED REACTIONS

As an application of effective Lagrangians, we calculate the reaction processes $\pi^- p \to K^- \Theta^+$ and $K^+ p \to \pi^+ \Theta^+$ via tree-level diagrams as shown in Fig. 5. These are alternative reactions to, for instance, photo-induced reactions, which are useful for further study of the Θ^+. The amplitudes for these reactions are given by

$$-it^s_{1/2^+}(\pi^- p \to K^- \Theta^+) = -it^s_{1/2^+}(K^+ p \to \pi^+ \Theta^+)$$
$$= i\frac{g^s_{1/2^+}}{2f}(-\sqrt{6})N_{\Theta^+}N_p, \tag{37}$$
$$-it^v_{1/2^+}(\pi^- p \to K^- \Theta^+) = it^v_{1/2^+}(K^+ p \to \pi^+ \Theta^+)$$
$$= i\frac{g^v_{1/2^+}}{4f^2}(-\sqrt{6})(2\sqrt{s} - M_\Theta - M_p)N_{\Theta^+}N_p F(k - k') \tag{38}$$

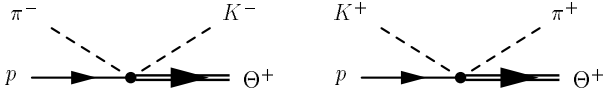FIG. 5: Feynman diagrams for the meson-induced reactions for Θ^+ production.
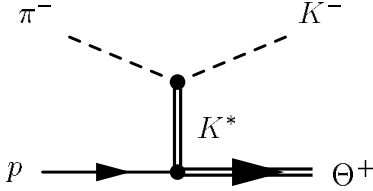

FIG. 6: Feynman diagram for the meson-induced reaction for Θ^+ production with a vector meson propagator.

for the $1/2^+$ case and by

$$
-it^s_{3/2^-}(\pi^- p \to K^- \Theta^+) = -it^s_{3/2^-}(K^+ p \to \pi^+ \Theta^+)
$$

$$
= i\frac{g^s_{3/2^-}}{4f^2}(-\sqrt{6})(\boldsymbol{k} - \boldsymbol{k}') \cdot \boldsymbol{S} N_{\Theta^+} N_p, \quad (39)
$$

$$
-it^v_{3/2^-}(\pi^- p \to K^- \Theta^+) = it^v_{3/2^-}(K^+ p \to \pi^+ \Theta^+)
$$

$$
= -i\frac{g^v_{3/2^-}}{4f^2}(-\sqrt{6})(\boldsymbol{k} + \boldsymbol{k}') \cdot \boldsymbol{S} N_{\Theta^+} N_p F(k - k')
$$

$$(40)$$

for the $3/2^-$ case, where the normalization factor is $N_i = \sqrt{(E_i + M_i)/2M_i}$, $\boldsymbol{S}$ is the spin transition operator, $\sqrt{s}$ is the initial energy, and k and k' are the momenta of the incoming and outgoing mesons, respectively. Here we define the vector meson propagator (Fig. 6) as

$$
F(k - k') = \frac{-m^2_{K^*}}{(k - k')^2 - m^2_{K^*} + im_{K^*}\Gamma[(k - k')^2]}, \quad (41)
$$

which is included in the vector-type amplitude. In the kinematical region in which we are interested, the momentum-dependent decay width of K^*, $\Gamma((k - k')^2)$ vanishes. Note that the scalar-type amplitude gives the same sign for $\pi^- p \to K^- \Theta^+$ and $K^+ p \to \pi^+ \Theta^+$, whereas the vector one gives opposite signs, reflecting the symmetry under exchange of two meson fields in the effective Lagrangians.

Since the two amplitudes must be summed coherently,

the squared amplitudes are given by

$$
\overline{\Sigma}\Sigma|t_{1/2^+}|^2 = \overline{\Sigma}\Sigma|t^s_{1/2^+} \pm t^v_{1/2^+}|^2
$$

$$
= 6\left(\frac{1}{2f}\right)^2 N^2_{\Theta^+} N^2_p \Big[(g^s_{1/2^+})^2 \pm 2g^s_{1/2^+} g^v_{1/2^+}
$$

$$
\times \frac{2\sqrt{s} - M_\Theta - M_p}{2f} F(k - k') + (g^v_{1/2^+})^2
$$

$$
\times \frac{(2\sqrt{s} - M_\Theta - M_p)^2}{4f^2} F^2(k - k')\Big], \quad (42)
$$

$$
\overline{\Sigma}\Sigma|t_{3/2^-}|^2 = 4\left(\frac{1}{4f^2}\right)^2 N^2_{\Theta^+} N^2_p \Big[(g^s_{3/2^-})^2(\boldsymbol{k} - \boldsymbol{k}')^2
$$

$$
\mp 2g^s_{3/2^-} g^v_{3/2^-}(|\boldsymbol{k}|^2 - |\boldsymbol{k}'|^2)F(k - k')
$$

$$
+ (g^v_{3/2^-})^2(\boldsymbol{k} + \boldsymbol{k}')^2 F^2(k - k')\Big], \quad (43)
$$

where $\pm$ and $\mp$ signs denote the $\pi^- p \to K^- \Theta^+$ and $K^+ p \to \pi^+ \Theta^+$ reactions, respectively. Notice that the relative phase between the two coupling constants is important, which affects the interference term of the two amplitudes. To determine the phase, we use the experimental information from $\pi^- p \to K^- \Theta^+$ reaction at KEK [16], where the upper limit of the cross section has been extracted to be a few μb.

The differential cross section for these reactions is given by

$$
\frac{d\sigma}{d\cos\theta}(\sqrt{s}, \cos\theta) = \frac{1}{4\pi s}\frac{|\boldsymbol{k}'|}{|\boldsymbol{k}|} M_p M_\Theta \frac{1}{2}\overline{\Sigma}\Sigma|t(\sqrt{s}, \cos\theta)|^2,
$$

$$(44)$$

which is evaluated in the center-of-mass frame. The total cross section can be obtained by integrating Eq. (44) with respect to $\cos\theta$:

$$
\sigma(\sqrt{s}) = \int_{-1}^1 d\cos\theta \frac{d\sigma}{d\cos\theta}(\sqrt{s}, \cos\theta).
$$

A. Qualitative analysis for $J^P = 1/2^+$ and $3/2^-$

Now let us calculate the cross section using the coupling constants obtained previously. In this section, we focus on the qualitative difference between $J^P = 1/2^+$ and $3/2^-$ cases. A more quantitative estimation of cross sections will be given in later sections.

We first calculate for the $1/2^+$ case, with coupling constants

$$
g^s_{1/2^+} = 0.47, \quad g^v_{1/2^+} = 0.47, \quad (45)
$$

where $g^s_{1/2^+}$ is one of the solutions that satisfies the condition (29). Since the result (25) spreads over a wide range, we choose $g^v_{1/2^+} = g^s_{1/2^+}$, which is well within the interval (30) determined from the self-energy. The result is shown in Fig. 7, with contributions from s and v terms. Each contribution is calculated by switching off the other
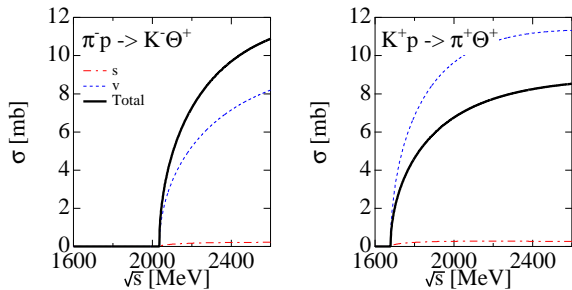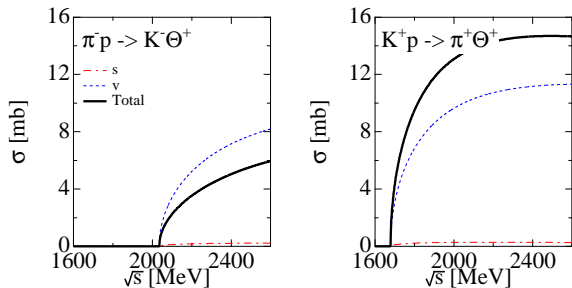
FIG. 7: (Color online) Total cross sections for the $J^P = 1/2^+$ case with $g^s = 0.47$ and $g^v = 0.47$. The thick line shows the result with full amplitude. Dash-dotted and dashed lines are the contributions from s and v terms, respectively.

FIG. 8: (Color online) Total cross sections for the $J^P = 1/2^+$ case with $g^s = 0.47$ and $g^v = -0.47$. The thick line shows the result with full amplitude. Dash-dotted and dashed lines are the contributions from s and v terms, respectively.

term. As we see, the use of the same coupling constant for both terms results in the dominance of the vector term. However, there is a sizable interference effect between s and v terms, although the contribution from the s term itself is small. The two amplitudes interfere constructively for the $\pi^- p \to K^- \Theta^+$ channel, whereas in the $K^+ p \to \pi^+ \Theta^+$ case they destructively interfere.

As already mentioned, the relative phase of the two coupling constants is not determined. If we change the sign,

$$g^s_{1/2^+} = 0.47, \quad g^v_{1/2^+} = -0.47, \qquad (46)$$

then the results change as in Fig. 8, where constructive and destructive interference appears in an opposite manner. It is worth noting that the amplitude for $\pi^- p \to K^- \Theta^+$ with the relative phase of Eq. (45) and that for $K^+ p \to \pi^+ \Theta^+$ with Eq. (46) are the same, as seen in Eq. (42). The difference only comes from the kinematic factors in cross section (44).

There is a preliminary result from KEK [16] that the cross section of $\pi^- p \to K^- \Theta^+$ was found to be very small, of the order of a few μb. At this stage, we do not want to calculate the cross section quantitatively, but the experimental result suggests that the relative phase of Eq. (46) should be plausible, for the small cross section
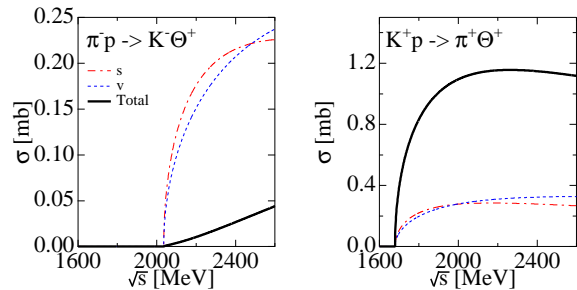

FIG. 9: (Color online) Total cross sections for the $J^P = 1/2^+$ case with $g^s = 0.47$ and $g^v = -0.08$, when the most destructive interference for $\pi^- p \to K^- \Theta^+$ takes place. Note that the vertical scale is different in the two panels. The thick line shows the result with full amplitude. Dash-dotted and dashed lines are the contributions from s and v terms, respectively.

for the $\pi^- p \to K^- \Theta^+$ reaction. In this case, the cross section for $K^+ p \to \pi^+ \Theta^+$ becomes large.

As a trial, let us search for the set of coupling constants with which the most destructive interference takes place in $\pi^- p \to K^- \Theta^+$, by changing $g^v_{1/2^+}$ within the interval (30). This means that the difference between cross sections of $\pi^- p \to K^- \Theta^+$ and $K^+ p \to \pi^+ \Theta^+$ is maximal. Then we find

$$g^s_{1/2^+} = 0.47, \quad g^v_{1/2^+} = -0.08. \qquad (47)$$

The result is shown in Fig. 9. A huge difference between $\pi^- p \to K^- \Theta^+$ and $K^+ p \to \pi^+ \Theta^+$ can be seen. In this case, we observe the ratio of cross sections

$$\frac{\sigma(K^+ p \to \pi^+ \Theta^+)}{\sigma(\pi^- p \to K^- \Theta^+)} \sim 50. \qquad (48)$$

Here we estimated the cross section σ as the average of the cross section shown in the figures (from threshold to 2.6 GeV). Notice that the ratio of the coupling constants $g^s_{1/2^+}/g^v_{1/2^+} \sim -5.9$ is relevant for the interference effect. It is possible to scale both coupling constants within experimental uncertainties. This does not change the ratio of cross sections, but it does change the absolute values.

Next we examine the case with $J^P = 3/2^-$. Again, we observe constructive and destructive interferences, depending on the relative sign of the two amplitudes. The interference effect is prominent around the energy region close to the threshold but is not very strong in the higher energy region, compared with $1/2^+$ case.

We search for the coupling constants with which the most destructive interference takes place for $\pi^- p \to K^- \Theta^+$. We find that destructive interference is maximized when the ratio of the coupling constants is $g^s_{3/2^-}/g^v_{3/2^-} \sim 0.5$. Taking, for instance, the values

$$g^s_{3/2^-} = 0.2, \quad g^v_{3/2^-} = 0.4, \qquad (49)$$

which are within the experimental bounds given in Sec. IV, we obtain the results shown in Fig. 10. In con-
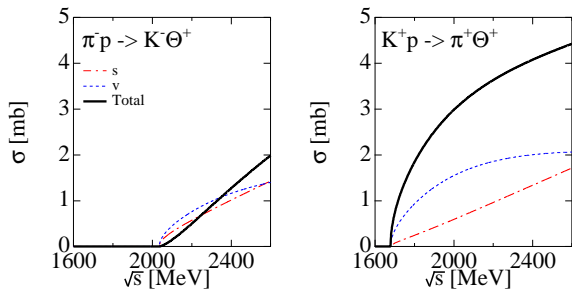
FIG. 10: (Color online) Total cross section for the $J^P = 3/2^-$ case with $g^s = 0.2$ and $g^v = 0.4$, when the most destructive interference for $\pi^- p \to K^- \Theta^+$ takes place. The thick line shows the result with full amplitude. Dash-dotted and dashed lines are the contributions from s and v terms, respectively.
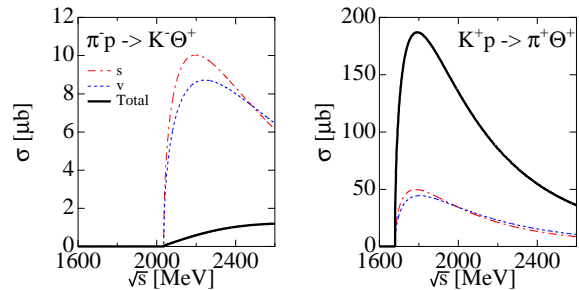

FIG. 11: (Color online) Total cross sections for the $J^P = 1/2^+$ case with $g^s = 0.47$ and $g^v = -0.08$, including a hadronic form factor (51). The thick line shows the result with full amplitude. Dash-dotted and dashed lines are the contributions from s and v terms, respectively.

trast to the $J^P = 1/2^+$ case, here the ratio of cross section is not very large:

$$\frac{\sigma(K^+ p \to \pi^+ \Theta^+)}{\sigma(\pi^- p \to K^- \Theta^+)} \sim 3.3. \tag{50}$$

The high-energy behavior in this case is understood from the p-wave nature of the coupling.

Let us mention the effect of the vector meson propagator. For simplicity, we take the same value for the coupling constants. First, we address the $J^P = 1/2^+$ case. Without introducing the vector meson propagator $F(k - k')$, the magnitude and energy dependence of the vector term is not similar to the scalar one, reflecting the structure of amplitudes (37) and (38). The difference between s and v amplitudes is $(2\sqrt{s} - M_\Theta - M_p)/2f$ with the same coupling constant, which ranges from 3 to 14 in the energy region under consideration. The cross section is proportional to its square, and therefore the vector term becomes the dominant one. The inclusion of the vector meson propagator reduces the cross section of the vector term, especially in the high-energy region. This eventually leads to the similar energy dependence of the two amplitudes t^s and t^v, resulting in a large cancellation between them, as seen in Fig. 9, although a factor $g^s_{1/2^+}/g^v_{1/2^+} \sim -5.9$ is still required to make the magnitude the same.

For the $J^P = 3/2^-$ case, without including the vector meson propagator, the scalar and vector contributions to the total cross section [the first and the third terms in Eq. (43)] become exactly the same, when we take the same coupling constant. Obviously, as seen in Eq. (43), the difference of the squared amplitudes is the term proportional to $\mathbf{k} \cdot \mathbf{k}' \propto \cos\theta$, which goes away when the angular integral is performed. This, however, does not lead to complete destructive interference, owing to the second term in Eq. (43). The vector meson propagator acts in the same way as before, and we obtain somehow a different energy dependence of the s and v results (Fig. 10) and a factor $g^s_{3/2^-}/g^v_{3/2^-} \sim 0.5$ to compensate for the reduction of the cross section of the vector term.

B. Hadronic form factor

Here we consider the reaction mechanism in detail to give a more quantitative result. First we introduce a hadronic form factor at the vertices, which accounts for the energy dependence of the coupling constants. Physically, it is understood as the reflection of the finite size of the hadrons. In practice, however, the introduction of the form factor has some ambiguities in its form and the cutoff parameters [20], which hopefully can be determined from experiment.

In Ref. [15], the $\pi^- p \to K^- \Theta^+$ reaction is studied with a three-dimensional monopole-type form factor

$$F(\sqrt{s}) = \frac{\Lambda^2}{\Lambda^2 + \mathbf{q}^2}, \tag{51}$$

where $\mathbf{q}^2 = \lambda(s, M_N^2, m_{in}^2)/4s$ with m_{in} being the mass of the incoming meson and $\Lambda = 0.5$ GeV. Here we adopt this form factor and apply it to the present process. We obtain the results for $J^P = 1/2^+$ in Fig. 11 and for $J^P = 3/2^-$ in Fig. 12, with the coupling constants given in Eqs. (47) and (49). With this form factor, the energy of the $K^+ p \to \pi^+ \Theta^+$ reaction of the ongoing experiment at KEK ($P_{\text{lab}} \sim 1200$ MeV, $\sqrt{s} \sim 1888$ MeV) is close to the maximum value for the cross section.

Notice that the ratio of the cross sections of $\pi^- p \to K^- \Theta^+$ and $K^+ p \to \pi^+ \Theta^+$ becomes larger than those of Eqs. (48) and (50). This is due to the use of the form factor (51), which contains the mass of the initial meson. It further contributes a factor ~ 2 for the ratio of $\pi^- p \to K^- \Theta^+$ and $K^+ p \to \pi^+ \Theta^+$.

We observe that the cross section is suppressed down to $\sim 1\mu$b for the $\pi^- p \to K^- \Theta^+$ reaction in the $1/2^+$ case. However, this is also a consequence of our choice of small coupling constants. Indeed, with these coupling constants, the self-energy of Θ^+ becomes

$$\text{Re}\Sigma^{1/2^+}_{\Theta^+} = \text{Re}\Sigma^s_{\Theta^+} + \text{Re}\Sigma^v_{\Theta^+} \sim -5.3 - 1.6 = -6.9 \text{ MeV,} \tag{52}$$

for $p^0 = 1700$ MeV and a cutoff 750 MeV. This is too small, but as we mentioned before, we can scale these
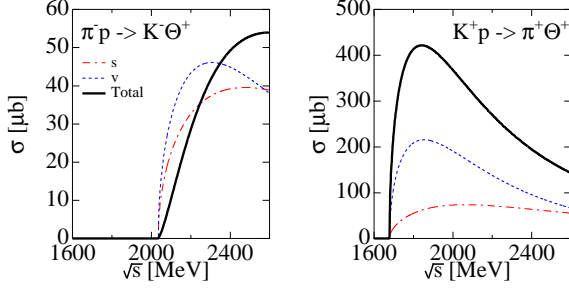
FIG. 12: (Color online) Total cross sections for the $J^P = 3/2^-$ case with $g^s = 0.2$ and $g^v = 0.4$, including a hadronic form factor (51). The thick line shows the result with full amplitude. Dash-dotted and dashed lines are the contributions from s and v terms, respectively.

constants without changing the ratio of $K^+p \to \pi^+\Theta^+$ and $\pi^-p \to K^-\Theta^+$. We would like to search for the coupling constants which provide a small cross section for $\pi^-p \to K^-\Theta^+$ reaction compatible with experiment and a moderate amount of self-energy, which guarantee the dominance of the two-meson coupling terms compared with the $KN\Theta^+$ vertex.

In Fig. 13, we plot the cross section of $\pi^-p \to K^-\Theta^+$ reaction and the self-energy of Θ^+ by fixing the ratio of coupling constants. The cross section is the value at $\sqrt{s} = 2124$ MeV, which corresponds to the KEK experiment $P_{\text{lab}} \sim 1920$ MeV. The horizontal line denotes the factor F, which is defined by

$$g^s_{1/2^+} = F \times 0.47, \quad g^v_{1/2^+} = -F \times 0.08. \quad (53)$$

We use $F = 1$ for the calculation of Fig. 11. Both the cross section and self-energy are proportional to the square of the coupling constant. Using the maximum value of cross section $\sim 4.1\mu$b [24] estimated by KEK experiment [16], we have

$$g^s_{1/2^+} = 1.59, \qquad g^v_{1/2^+} = -0.27, \quad (54)$$
$$\sigma_{\pi^-p \to K^-\Theta^+} = 4.1\mu\text{b}, \qquad \text{Re}\Sigma_\Theta = -78 \text{ MeV}.$$

Furthermore, if we use the upper limit of the scalar term of the coupling constant, we fix

$$g^s_{1/2^+} = 1.37, \qquad g^v_{1/2^+} = -0.23, \quad (55)$$
$$\sigma_{\pi^-p \to K^-\Theta^+} = 3.2\mu\text{b}, \qquad \text{Re}\Sigma_\Theta = -58 \text{ MeV}.$$

However, if we want to obtain $\text{Re}\Sigma_\Theta = -100$ MeV, we have

$$g^s_{1/2^+} = 1.80, \qquad g^v_{1/2^+} = -0.31, \quad (56)$$
$$\sigma_{\pi^-p \to K^-\Theta^+} = 5.0\mu\text{b}, \qquad \text{Re}\Sigma_\Theta = -100 \text{ MeV}.$$

We see that a sizable self-energy is obtained with the coupling constants (54) and (56). These results are summarized in Table II.

TABLE II: Summary of the coupling constants, cross sections and self-energies. σ_{π^-} is the total cross section for $\pi^-p \to K^-\Theta^+$ are the values at $P_{\text{lab}} = 1920$ MeV; σ_{K^+} is that for $K^+p \to \pi^+\Theta^+$, which is the upper limit of the cross section at $P_{\text{lab}} = 1200$ MeV.

J^P	g^s	g^v	σ_{π^-} [μb]	σ_{K^+} [μb]	$\text{Re}\Sigma_\Theta$ [MeV]
$1/2^+$	1.59	-0.27	4.1	<1928	-78
	1.37	-0.23	3.2	<1415	-58
	1.80	-0.31	5.0	<2506	-100
$3/2^-$	0.104	0.209	4.1	< 113	-23
	0.125	0.25	5.9	< 162	-32
	0.22	0.44	18	< 502	-100

For the $J^P = 3/2^-$ case, with $g^s_{3/2^-} = 0.2$ and $g^v_{3/2^-} = 0.4$, the self-energy of Θ^+ becomes

$$\text{Re}\Sigma_{\Theta^+}^{3/2^-} = \text{Re}\Sigma^s_{\Theta^+} + \text{Re}\Sigma^v_{\Theta^+} \sim -4 - 80 = -84 \text{ MeV}. \quad (57)$$

In Fig. 13, we plot the cross section of the $\pi^-p \to K^-\Theta^+$ reaction and the self-energy of Θ^+ by fixing the ratio of coupling constants. The horizontal line denotes the factor F, which is defined by

$$g^s_{1/2^+} = F \times 0.2, \quad g^v_{1/2^+} = F \times 0.4. \quad (58)$$

Using the maximum value of cross section $\sim 4.1\mu$b estimated by the KEK experiment, we have

$$g^s_{3/2^-} = 0.104, \qquad g^v_{3/2^-} = 0.209, \quad (59)$$
$$\sigma_{\pi^-p \to K^-\Theta^+} = 4.1\mu\text{b}, \qquad \text{Re}\Sigma_\Theta = -23 \text{ MeV}.$$

In the region plotted in the figure, the coupling constants do not exceed the upper bounds, but the lower limit of $g^v_{3/2^-}$ appears:

$$g^s_{3/2^-} = 0.125, \qquad g^v_{3/2^-} = 0.25, \quad (60)$$
$$\sigma_{\pi^-p \to K^-\Theta^+} = 5.9\mu\text{b}, \qquad \text{Re}\Sigma_\Theta = -33 \text{ MeV}.$$

To make $\text{Re}\Sigma_\Theta = -100$ MeV, we have

$$g^s_{3/2^-} = 0.22, \qquad g^v_{3/2^-} = 0.44, \quad (61)$$
$$\sigma_{\pi^-p \to K^-\Theta^+} = 18\mu\text{b}, \qquad \text{Re}\Sigma_\Theta = -100 \text{ MeV}.$$

Finally, we show the angular dependence of the cross sections. In Figs. 14 and 15, we plot the angler dependence of the differential cross sections at the energy of KEK experiment: $P_{\text{lab}} \sim 1920$ MeV for $\pi^-p \to K^-\Theta^+$ and $P_{\text{lab}} \sim 1200$ MeV for $K^+p \to \pi^+\Theta^+$. For the $J^P = 1/2^+$ case, the contribution from the s term has no angular dependence, whereas the v term shows a forward peak, owing to the t-channel exchange of the vector meson propagator. Because of the interference of the two amplitudes, the total result becomes zero at $\cos\theta \sim 0.5$ for the $\pi^-p \to K^-\Theta^+$ reaction. For the $J^P = 3/2^-$ case, the s term varies linearly in $\cos\theta$, leading to a backward peak. The v term shows a forward peak, which is enhanced by the vector meson propagator. Interference of the two amplitude leads to a clear forward peak for both $\pi^-p \to K^-\Theta^+$ and $K^+p \to \pi^+\Theta^+$ reactions.
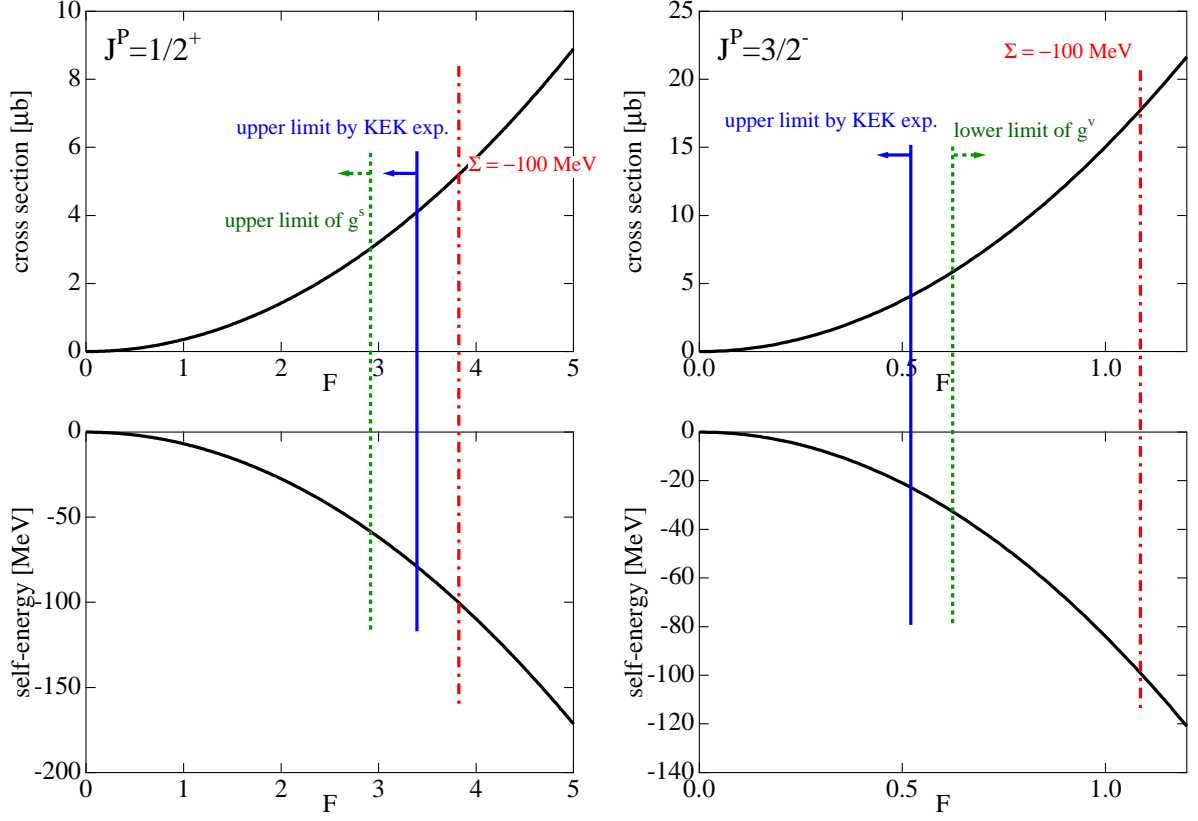
FIG. 13: (Color online) The total cross section of $\pi^- p \to K^- \Theta^+$ at $P_{\text{lab}} = 1920$ MeV and the real part of the self-energy of Θ^+ as functions of the factor F defined in Eqs. (53) and (58) for $J^P = 1/2^+$ (left) and $J^P = 3/2^-$ (right). Solid, dashed and dash-dotted vertical lines show the upper limit of cross section given by the KEK experiment [16], the limit of coupling constant, and the point where $\text{Re}\Sigma = -100$ MeV.
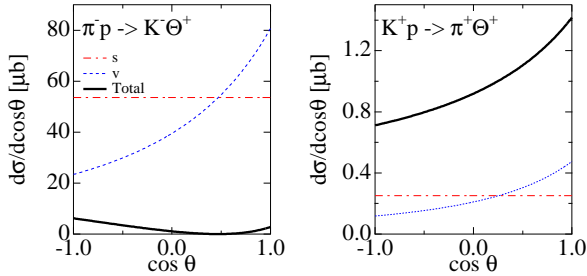

FIG. 14: (Color online) Angular dependence of the differential cross section for $\pi^- p \to K^- \Theta^+$ at $P_{\text{lab}} \sim 1920$ MeV (left) and for $K^+ p \to \pi^+ \Theta^+$ at $P_{\text{lab}} \sim 1200$ MeV (right) for the $J^P = 1/2^+$ case with $g^s = 1.59$ and $g^v = -0.27$, including a hadronic form factor (51). The thick line shows the result with full amplitude. Dash-dotted and dashed lines are the contributions from s and v terms, respectively.

FIG. 15: (Color online) Angular dependence of the differential cross section for $\pi^- p \to K^- \Theta^+$ at $P_{\text{lab}} \sim 1920$ MeV (left) and for $K^+ p \to \pi^+ \Theta^+$ at $P_{\text{lab}} \sim 1200$ MeV (right) for the $J^P = 3/2^-$ case with $g^s = 0.106$ and $g^v = 0.212$, including a hadronic form factor (51). The thick line shows the result with full amplitude. Dash-dotted and dashed lines are the contributions from s and v terms, respectively.

C. Effect of Born terms

In this subsection, we briefly discuss the possible effect from the Born terms, as shown in Fig. 16, which
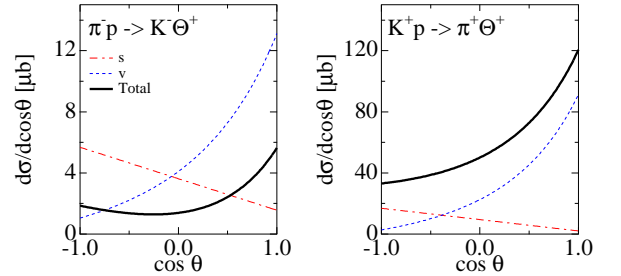
have not been taken into account in the present studies. However, there are reasons that the Born terms are not important in the present reactions. First, the Born terms are proportional to the decay width of Θ^+ and therefore suppressed if the decay width of the Θ^+ is nar-
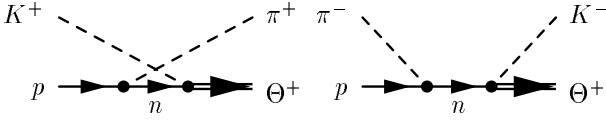
FIG. 16: Born terms for the reaction: u-channel diagram for $K^+p \to \pi^+\Theta^+$ (left); s-channel diagram for $\pi^-p \to K^-\Theta^+$ (right).

row. Second, in the energy region of Θ^+ production, the energy denominator of the exchanged nucleon suppresses the contribution, especially for the s-channel term in the $\pi^-p \to K^-\Theta^+$ reaction. Here we would like to confirm this explicitly.

At the tree level, there are s-, t-, and u-channel diagrams. However, assuming $I = 0$ for Θ^+, there is only a u channel in $K^+p \to \pi^+\Theta^+$ (Fig. 16, left), whereas there is only an s channel in $\pi^-p \to K^-\Theta^+$ (Fig. 16, right). For these terms, we need the Yukawa couplings such as $KN\Theta^+$ and πNN couplings. There are two schemes to introduce the Yukawa couplings, namely, pseudoscalar (PS) and pseudovector (PV) schemes. For the construction of the Born amplitude, it is reasonable to rely on chiral symmetry, where the two schemes should provide the same results.

In this case the meson-baryon scattering amplitude should be a quantity of $\mathcal{O}(k)$ or higher, where k is a momentum of mesons. In the PV scheme, since each $KN\Theta$ coupling is of $\mathcal{O}(k)$, the Born amplitude behaves as $\mathcal{O}(k^2)$, consistent with this observation. In contrast, a naive construction of the Born term in the PS scheme leads to an amplitude of $\mathcal{O}(1)$. It is well-known that a scalar exchange term cancel the term of $\mathcal{O}(1)$. However, the interaction of the scalar channel is not well understood. Therefore, we adopt the PV scheme in the following study. Another advantage of the PV scheme is that it can be extended easily to the $J^P = 3/2^-$ case, while it is not so simple in the PS scheme [21]. In this respect, our method differs from the previous study of similar reactions [14, 15], in which the PS scheme was used.

The interaction Lagrangians for $1/2^+$ are

$$\mathcal{L}_{KN\Theta}^{1/2^+} = \frac{g_A^{*,1/2^+}}{2f}\bar{\Theta}^+\gamma_\mu\gamma_5\partial^\mu KN + \text{h.c.}, \qquad (62)$$

$$\mathcal{L}_{\pi NN} = \frac{g_A}{2f}\bar{N}\gamma_\mu\gamma_5\partial^\mu\boldsymbol{\pi}N. \qquad (63)$$

The fields N and $\boldsymbol{\pi}$ are defined in Eq. (7), and the Kaon field is defined as

$$K = \begin{pmatrix} -K^0 & K^+ \end{pmatrix}, \qquad (64)$$

and the coupling constants are determined as

$$g_A^{*,1/2^+} = 0.0935, \qquad (65)$$

which is determined by $\Gamma_{\Theta^+} = 1$ MeV, and we use
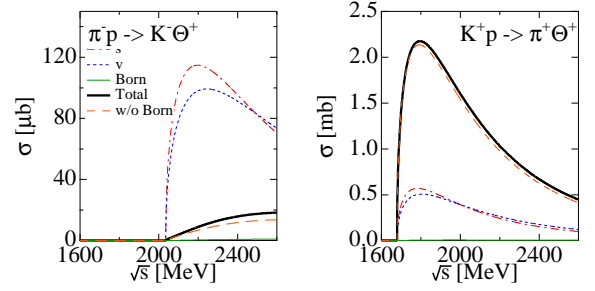
$$g_A = 1.25. \qquad (66)$$

FIG. 17: (Color online) Total cross section for the $J^P = 1/2^+$ case with $g^s = 1.59$ and $g^v = -0.27$, including hadronic form factor (51) and Born terms. The thick line shows the result with full amplitude. Dash-dotted, dashed, and thin lines are the contributions from s, v, and Born terms, respectively. The result without Born terms are shown by the long-dashed lines.

The amplitude for $\pi^-(k)p(p) \to K^-(k')\Theta^+(p')$ is given by

$$-it = i\sqrt{2}\frac{g_A^{*,1/2^+} g_A}{4f^2}(\boldsymbol{\sigma}\cdot\boldsymbol{k}')\frac{M}{E}\frac{1}{p_0 + k_0 - E(\boldsymbol{p}+\boldsymbol{k})}(\boldsymbol{\sigma}\cdot\boldsymbol{k}),$$

and for $K^+(k)p(p) \to \pi^+(k')\Theta^+(p')$,

$$-it = i\sqrt{2}\frac{g_A^{*,1/2^+} g_A}{4f^2}(\boldsymbol{\sigma}\cdot\boldsymbol{k})\frac{M}{E}\frac{1}{p_0 - k_0' - E(\boldsymbol{p}-\boldsymbol{k}')}(\boldsymbol{\sigma}\cdot\boldsymbol{k}').$$

In Fig. 17 we show the results including Born terms. We can observe that the effect of Born terms is indeed small in both reactions.

For the $J^P = 3/2^-$ case, the interaction Lagrangian can be written as

$$\mathcal{L}_{KN\Theta}^{3/2^-} = \frac{g_A^{*,3/2^-}}{2f}\bar{\Theta}^{+\mu}\gamma_5\partial_\mu KN + \text{h.c.}, \qquad (67)$$

with the same πNN vertex in Eq. (66). In the nonrelativistic expansion this term yields a d-wave coupling so that the square of momenta appears in the vertex. It reduces the contribution further than the $1/2^+$ case, and therefore, the effect of Born terms for $J^P = 3/2^-$ is also small.

VI. SUMMARY

In this paper, we studied the two-meson couplings of Θ^+ for $J^P = 1/2^+$ and $3/2^-$. The effective interaction Lagrangians for the two-meson coupling were given, and these coupling constants were determined based on the **8-$\overline{\mathbf{10}}$** representation mixing scheme, by using information of the $N^* \to \pi\pi N$ decays. These values were further constrained in order to provide appropriate size of the self-energy of the Θ^+. Finally, we applied the effective Lagrangian to the meson induced reactions $\pi^-p \to K^-\Theta^+$ and $K^+p \to \pi^+\Theta^+$.

We found that there is an interference effect between the two amplitudes of the scalar and vector types, which can help to explain the very small cross section for the $\pi^- p \to K^- \Theta^+$ reaction observed at KEK [16]. In this case, reflecting the symmetry under exchange of two amplitudes, the large cross section for $K^+ p \to \pi^+ \Theta^+$ reaction was obtained as a consequence of the interference. The interference occurs in both $1/2^+$ and $3/2^-$ cases.

In Table II, we summarize the results obtained in the present analysis. For a given set of coupling constants, the upper bound of the cross section of the $K^+ p \to \pi^+ \Theta^+$ reaction is estimated by maximizing the interference effect. We observe that the large cross section of the order of millibarns for $K^+ p \to \pi^+ \Theta^+$ is obtained for the $1/2^+$ case, whereas the upper limit of the cross section is not very large for $3/2^-$ case. Therefore, if large cross sections are observed in the $K^+ p \to \pi^+ \Theta^+$ reaction, it would indicate $J^P = 1/2^+$ for the Θ^+.

For completeness, we would like to mention the case where the cross sections for both $\pi^- p \to K^- \Theta^+$ and $K^+ p \to \pi^+ \Theta^+$ reactions are small. If the cross section of $K^+ p \to \pi^+ \Theta^+$ reaction is also small, it could be explained by the small coupling constants and is not an interference effect. For the $J^P = 1/2^+$ case, both coupling constants can be zero within the experimental uncertainties. However, for the $3/2^-$ case, there is a lower limit for the $g^v_{3/2^-}$, which means that the lower limit is also imposed for the cross sections. We search for the set of coupling constants that provide the minimum value for the $K^+ p \to \pi^+ \Theta^+$ cross section, keeping

a $\pi^- p \to K^- \Theta^+$ cross section to be less than 4.1μb. We obtain $\sigma_{K^+ p \to \pi^+ \Theta^+} \sim 58 \mu$b with $g^s_{3/2^-} = 0.04$ and $g^v_{3/2^-} = 0.18$. However, one should notice that the small coupling constants do not guarantee the dominance of two-meson coupling, and the Born terms and interference effect may play a role, which is beyond our present scope.

The present analysis provides an extension of effective interactions obtained in Ref. [22] with representation mixing and $J^P = 3/2^-$. It is also interesting to apply the present extension to the study of the medium effect of Θ^+ [22] and the production of Θ^+ hypernuclei [23]. From the experimental point of view, the cross section of $K^+ p \to \pi^+ \Theta^+$ reaction is of particular importance to the present results. To perform a better analysis for the two-meson coupling, more experimental data for three-body decays of nucleon resonances are strongly desired.

[1] LEPS, T. Nakano *et al.*, Phys. Rev. Lett. **91**, 012002 (2003).
[2] K. H. Hicks, Prog. Part. Nucl. Phys. **55**, 647 (2005).
[3] P. Bicudo and G. M. Marques, Phys. Rev. D **69**, 011503(R) (2004).
[4] T. Kishimoto and T. Sato, hep-ex/0312003.
[5] F. J. Llanes-Estrada, E. Oset, and V. Mateu, Phys. Rev. C **69**, 055203 (2004).
[6] P. Bicudo, Phys. Rev. D **70**, 111504(R) (2004).
[7] F. Huang, Z. Y. Zhang, and Y. W. Yu, hep-ph/0411222.
[8] A. Hosaka, T. Hyodo, F.J. Llanes-Estrada, E. Oset, J. R. Peláez, and M. J. Vicente Vacas, Phys. Rev. C **71**, 045205 (2005).
[9] D. P. Roy, J. Phys. G **30**, R113 (2004).
[10] T. Hyodo and A. Hosaka, Phys. Rev. D **71**, 054017 (2005).
[11] A. Hosaka, M. Oka, and T. Shinozaki, Phys. Rev. D **71**, 074021 (2005).
[12] T. Hyodo, A. Hosaka, and E. Oset, Phys. Lett. **B579**, 290 (2004).
[13] W. Liu and C. M. Ko, Phys. Rev. C **68**, 045203 (2003).
[14] Y. Oh, H. Kim, and S. H. Lee, Phys. Rev. D **69**, 074016 (2004).
[15] Y.-s. Oh, H.-c. Kim, and S. H. Lee, Phys. Rev. D **69**, 014009 (2004).
[16] K. Imai, Talk given at Exotic Hadrons Workshop, May 27, 2005; http://www.hepl.phys.nara-wu.ac.jp/exohad05/files/exohad05_imai.pdf, K. Miwa (private communication).
[17] Particle Data Group, S. Eidelman *et al.*, Phys. Lett. **B592**, 1 (2004).
[18] W. Rarita and J. S. Schwinger, Phys. Rev. **60**, 61 (1941).
[19] S. Theberge, A. W. Thomas, and G. A. Miller, Phys. Rev. D **22**, 2838 (1980).
[20] S. I. Nam, A. Hosaka, and H. C. Kim, Phys. Lett. **B579**, 43 (2004).
[21] S.-I. Nam, A. Hosaka, and H.-C. Kim, Phys. Rev. D **71**, 114012 (2005).
[22] D. Cabrera, Q. B. Li, V. K. Magas, E. Oset, and M. J. Vicente Vacas, Phys. Lett. **B608**, 231 (2005).
[23] H. Nagahiro, S. Hirenzaki, E. Oset, and M. J. Vicente Vacas, Phys. Lett. **B620**, 125 (2005).
[24] The upper limit $\sim 4.1 \mu$b is determined by assuming the isotropic decay of $\Theta^+ \to KN$ [16]. In our calculation, the angular dependence of the decay is not very large, as shown in the following. Therefore we simply use this value for the estimation of upper limit here.